Field repeatability of a low-cost permanent seismic system for 4D monitoring

Xinding Fang[*1,2], *Siwei Li*[1], *Tianrun Chen*[1], and *Nicholas Brooks*[1]
[1]*SensorEra Inc.;* [2]*Department of Earth and Atmospheric Sciences, University of Houston.*

Summary

This study evaluates the field repeatability of a low-cost permanent seismic monitoring system using six months of repeated Surface Linear Vibrator (SLV) data acquired at our Needville test site in Texas. Two permanently buried geophones, located 473 m from the source, recorded repeat surveys approximately every three days from January through June 2026. This dense baseline dataset captures a broad range of weather-driven near-surface conditions and provides a practical basis for quantifying the acquisition noise floor of a sparse permanent 4D monitoring system. The results support three main conclusions. First, deep geophone burial is essential for high-quality time-lapse recording because it substantially reduces weather-related near-surface contamination. Second, a dedicated 4D de-noising workflow can suppress a large fraction of unrepeatable noise when reflection energy dominates the selected analysis windows. Third, co-located weather records are critical for interpreting time-lapse variations, identifying surface-sensitive time windows, and distinguishing short-lived weather anomalies from slower reservoir-scale responses. For the deep geophone, raw normalized root-mean-square (NRMS) differences of approximately 10–50% are reduced to about 10% after de-noising, and residual monitor-to-baseline time shifts are generally limited to ±0.2 ms. Weather-driven anomalies exhibit a distinctive signature—abrupt onset following rainfall and decay over days to weeks—that separates them from the gradual drift expected from reservoir-scale processes. These results provide guidance for baseline characterization, pre-survey detectability analysis, and permanent 4D system design.

Introduction

Permanent seismic monitoring is increasingly attractive for carbon storage, geothermal development, hydrocarbon production, and other subsurface applications that require repeated measurements over long periods. Compared with crew-based repeat surveys, a permanent source-receiver system can acquire data frequently and with fixed geometry, reducing operational variability and enabling interpretation based on temporal trends rather than a small number of isolated survey vintages. The practical challenge is that high temporal sampling also reveals repeatability variations caused by the near surface. Rainfall, soil-moisture changes, temperature fluctuations, and seasonal wetting and drying can modify shallow velocity and attenuation, producing amplitude changes, phase shifts, and wave-path perturbations that may mask or mimic true reservoir 4D responses.

The objective of this study is to quantify the field repeatability of a low-cost permanent seismic system (Contenti et al., 2025; Li et al., 2023; Li et al., 2025; Verliac et al., 2026) and to evaluate how effectively processing can reduce time-lapse variations caused by seasonal near-surface changes. The Needville baseline experiment leads to three practical lessons: (1) deeply buried geophones are required to obtain repeatable, reflection-dominated data; (2) the proposed de-noising approach can remove a substantial portion of 4D noise when the near-surface contribution is secondary; and (3) interpretation must be supported by local weather observations so that rainfall-sensitive time windows and seasonally variable receiver behavior are identified and documented before reservoir-related changes are interpreted.

Field experiment setup

The field experiment was conducted at our Needville test site using a permanently installed SLV source and two buried vertical-component geophones. Source-receiver geometry was fixed throughout the experiment, minimizing geometry-related repeatability errors and allowing the study to focus on source stability, receiver burial depth, processing performance, and environmental variability. The shallow and deep geophones were buried at about 11 m (36 ft) and 16 m (52.5 ft), respectively. These depths were selected to compare a relatively near-surface installation with a deeper installation that is less affected by weathering-layer variations. Borehole coring indicates that the near-surface formation transitions from unconsolidated sand to consolidated clay at a depth of about 11 m. Notably, both receivers were buried much deeper than typical industry practice, where permanent receivers are commonly buried at 1-3 m. The 473 m offset is representative of the source-receiver spacing used in our sparse production arrays, so the measured noise floor is directly applicable to operational system design.

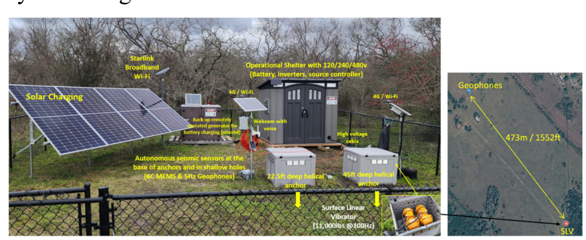

Figure 1: Field setup for the SLV source and buried geophones.

Repeat surveys were acquired approximately every three days from January 5 to June 28, 2026. Each survey consisted of 100 source sweeps. Each sweep included a 3 s up-sweep followed by a 27 s down-sweep, with a peak frequency of 65 Hz (Figure 2). The surveys were acquired near midnight to reduce cultural noise and minimize the influence of diurnal temperature variations.

For each sweep, the processed geophone trace was obtained by cross-correlating the recorded data with the source wavelet measured by a vibration sensor mounted on the source anchor, followed by deconvolution to remove the source signature. Because the source wavelet was measured independently for every sweep, variations in source-ground coupling associated with changing near-surface conditions were compensated during processing. Figure 2 shows 100 pre-stack processed sweeps recorded by the deep geophone during one survey. The average cross-correlation coefficient between sweep pairs is 99.7%, indicating excellent within-survey repeatability and stable source performance. This high level of consistency is also maintained between adjacent surveys acquired under stable weather conditions.

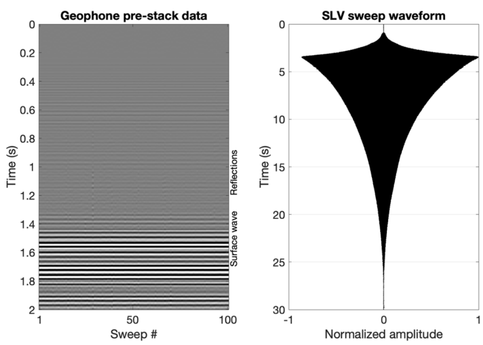

Figure 2: A gather of 100 pre-stack processed sweeps recorded by the deep geophone during a single survey (left) and the source sweep waveform recorded by the source vibration sensor (right).

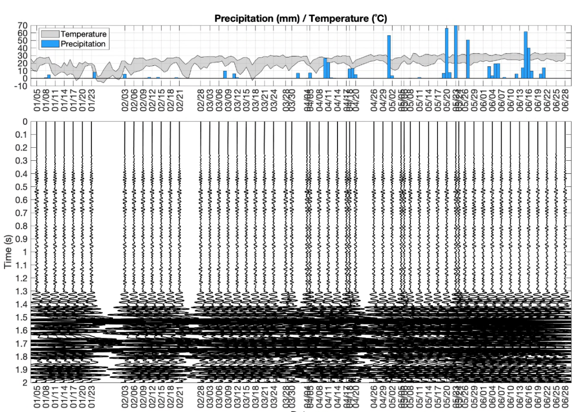

Figure 3: Time-lapse gather of 57 survey-day stacked traces recorded by the deep geophone between January 5 and June 28, 2026. The top weather panel shows rainfall and temperature variations. The strongest late arrivals after approximately 1.3 s are surface waves and are excluded from the main repeatability analysis.

Figure 3 shows 57 survey-day stacked traces acquired during the monitoring period, with each trace formed by stacking 100 processed sweeps. A local weather station installed on 2/22 recorded rainfall, temperature, and other environmental parameters at the test site. Prior to its installation, weather data were obtained from the nearby public weather station KSGR0. Because no injection or production occurred during the monitoring period, the observed time-lapse variations are interpreted as the response of the shallow subsurface to seasonal near-surface changes.

Data analysis and 4D de-noising workflow

The analysis was performed in reflection-dominated time windows above approximately 1.3 s, excluding the dominant surface-wave train. Within these windows, the recorded data are treated as a superposition of deep reflection energy and shallow-propagating energy, as illustrated in Figure 4. Reflections from the target depth (or reservoir), overburden, and underlying layers travel mainly along near-vertical ray paths and are therefore less sensitive to lateral variations in the shallow subsurface. By contrast, direct arrivals, shallow diving waves, shallow multiples, diffractions from near-surface heterogeneities, and surface waves propagate more laterally and are more sensitive to soil moisture and weathering-layer velocity changes.

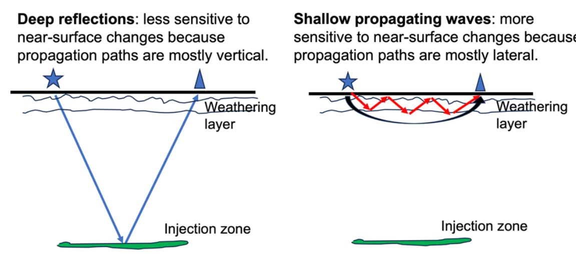

Figure 4: Conceptual separation of deep reflections and shallow-propagating waves. Deep reflections traverse the weathering layer along near-vertical ray paths and are therefore less sensitive to lateral near-surface variations, whereas shallow-propagating waves travel predominantly laterally and are more strongly affected by changes in the weathering layer.

For a given acquisition time t_A, the data recorded by a receiver in a local time window can be written conceptually in the frequency domain as

$$D(\omega, t_A) = H(\omega, t_A) \cdot R(\omega, t_A) + S(\omega, t_A) \quad (1)$$

where $D(\omega, t_A)$ is the recorded data, $R(\omega, t_A)$ is the deep reflection response, $H(\omega, t_A)$ is a transfer function that represents the near-surface filtering effect common to deep reflections, $S(\omega, t_A)$ is the shallow-propagating wavefield, and ω is angular frequency.

The processing objective is not to force every monitor trace to match the baseline, but to suppress components that are inconsistent with the reflection-dominated response while preserving residual phase and amplitude variations that may represent true subsurface changes. For reflections from the target depth or deeper formations, the acquisition time dependence of $R(\omega, t_A)$ can be approximated locally as a phase shift,

$$R(\omega, t_A) \approx R_0(\omega) \cdot e^{-i\omega\Delta\tau_A} \quad (2)$$

where $\Delta\tau_A$ is the travel-time delay or advance associated with subsurface velocity changes. We further assume that, in the selected windows, deep reflections dominate the recorded data and the shallow-propagating wavefield is a secondary contribution. Under these assumptions, the de-noising workflow estimates the repeatable reflection component and suppresses acquisition-related 4D noise associated with $H(\omega, t_A)$ and $S(\omega, t_A)$, while retaining residual variations that are coherent in time and consistent with reflection behavior. Note that the phase-shift approximation in Equation (2) is used only for the waveform alignment step of the workflow. Residual amplitude variations, which often represent the primary seismic response to CO_2 plume migration or reservoir changes through amplitude brightening, are preserved rather than suppressed.

Results

NRMS and monitor-to-baseline time shift were used to evaluate time-lapse repeatability. The January 5 survey was used as the baseline, and all later surveys were treated as monitors. Both attributes were calculated with a 0.1 s sliding window, allowing the repeatability behavior to be examined as a function of both calendar time and seismic arrival time.

For the raw deep-geophone data (Figure 5), NRMS generally ranges from 10% to 50%, with the largest anomalies occurring after the major rainfall events on May 2 and May 20–23 (Figure 3). Smaller anomalies are also observed after rainfall in March and April. The time-shift maps show similar temporal patterns, indicating that rainfall-induced near-surface velocity changes affect both waveform amplitude and phase. Unlike the gradual response expected from CO_2 plume migration or other reservoir-scale processes, these weather-related anomalies appear abruptly and decay over days to weeks.

After 4D de-noising, the repeatability of the deep-geophone data improves substantially (Figure 6). NRMS is reduced to approximately 10% over most reflection windows, and residual time shifts are generally confined to within ±0.2 ms. Figure 7 compares the data before and after de-noising and shows that the removed component is generally small relative to the reflection signal. These results indicate that the dominant 4D noise can be effectively suppressed when reflections dominate the analysis window and the shallow-propagating wavefield remains secondary.

Some windows retain coherent residual anomalies after processing. In this baseline experiment, these anomalies are more likely to represent surface-sensitive intervals than changes at the target depth because no injection or production occurred. Such intervals should be evaluated with local weather records and temporal consistency tests before being used for 4D interpretation.

The shallow-geophone results (Figures 8 and 9) provide an important contrast. After rainfall, the shallow receiver exhibits much larger NRMS and time-shift variations, with raw NRMS ranging from 10% to 100%, residual NRMS exceeding 50% over broad time windows after de-noising, and residual time shifts greater than ±1 ms. The same de-noising workflow cannot fully remove these near-surface effects. This contrast demonstrates that de-noising effectiveness is governed by the ratio of reflection energy to near-surface energy, which is controlled primarily by acquisition design rather than processing. Sensor burial depth is therefore a key factor controlling time-lapse repeatability and the reliability of 4D interpretation.

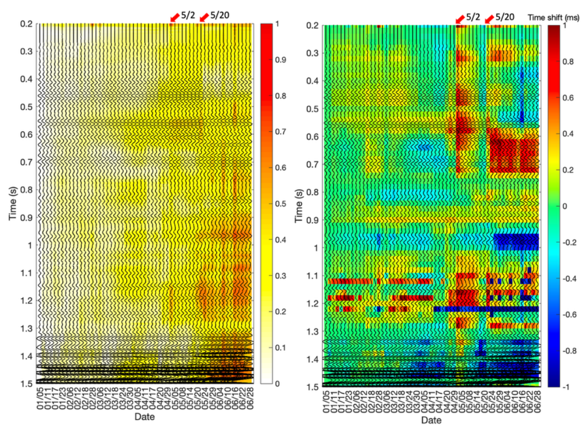

Figure 5: NRMS (left) and time shift (right) of the deep geophone raw data before 4D de-noising.

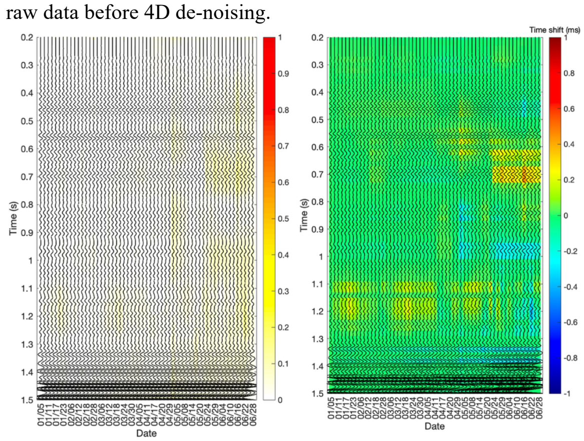

Figure 6: NRMS (left) and time shift (right) of the deep geophone data after 4D de-noising.

4D repeatability of the SLV system

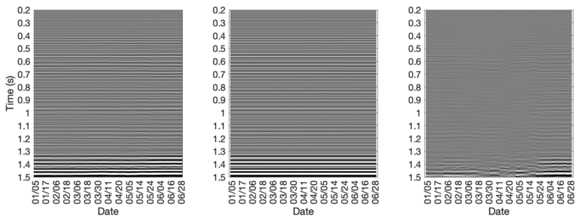

Figure 7: Time-lapse gathers before 4D de-noising (left), after 4D de-noising (middle), and the removed 4D noise component (right).

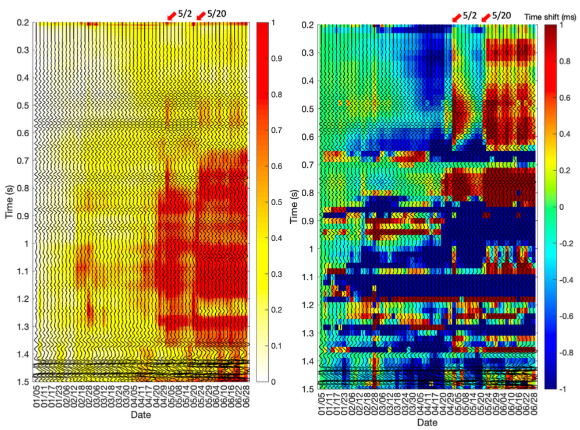

Figure 8: NRMS (left) and time shift (right) of the shallow geophone raw data before 4D de-noising.

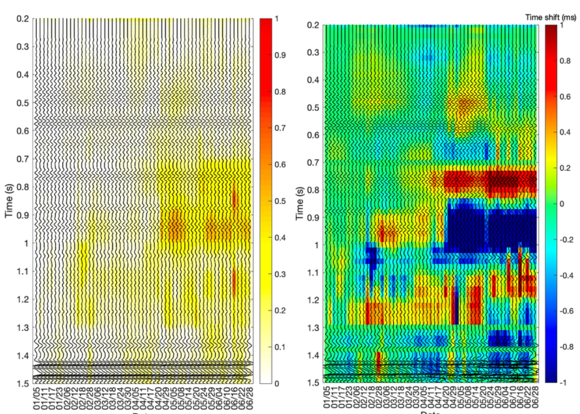

Figure 9: NRMS (left) and time shift (right) of the shallow geophone data after 4D de-noising.

Discussion

The Needville experiment demonstrates that dense temporal sampling and local weather observations are essential for reliable permanent 4D monitoring. Without rainfall records, the abrupt anomalies observed in May could be misinterpreted as subsurface changes. With local weather observations, these anomalies can be identified as near-surface responses and used to classify surface-sensitive time windows. This is particularly important for sparse permanent arrays, where each source-receiver pair samples a distinct near-surface path and may respond differently to rainfall, drying, and seasonal temperature variations.

A practical monitoring program should include a baseline period of 6–12 months to characterize seasonal variability before injection or production effects become dominant. This baseline supports estimation of the acquisition noise floor, identification of stable reflection windows, validation of the de-noising workflow, and determination of detectability thresholds for each source-receiver pair. Pair-specific characterization is essential: a single global noise model may under-correct contaminated windows, leaving weather artifacts, or over-correct stable windows, suppressing genuine 4D signals.

The results also highlight the complementary roles of acquisition design and processing. De-noising can reduce repeatability noise, but it cannot compensate for receiver installations dominated by near-surface wavefields. The best performance is achieved by first minimizing near-surface sensitivity through acquisition design and then applying targeted de-noising to the remaining repeatability noise. Deep geophone burial, fixed-geometry acquisition, local weather monitoring, and targeted de-noising should therefore be treated as complementary components of a permanent 4D monitoring strategy.

Conclusion

Six months of repeated seismic surveys at the Needville test site demonstrate that deeply buried geophones are essential for reliable permanent 4D monitoring. Compared with the shallow geophone, the deep geophone records reflection-dominated data with substantially less weather-related contamination. This enables the proposed de-noising workflow to reduce NRMS to approximately 10% and limit residual time shifts to within ±0.2 ms over most reflection windows. These values define a practical noise floor comparable to published detection thresholds for early-stage CO_2 plume anomalies, indicating that the system can resolve reservoir-scale time-lapse signals once weather-driven effects are accounted for. Local weather observations are indispensable for distinguishing near-surface effects from potential subsurface changes and for identifying weather-sensitive time windows. A practical implication is that permanent monitoring programs should include a 6-12 month pre-injection baseline period to characterize seasonal variability, establish pair-specific detectability thresholds, and validate the de-noising workflow before injection effects become dominant. Together, these results establish the practical acquisition noise floor of the system and provide a framework for assessing time-lapse detectability before deployment in active reservoir or CO_2 storage monitoring.